

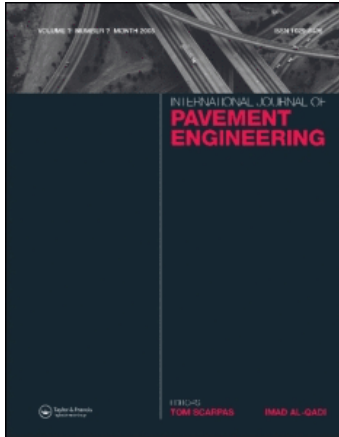
This article was downloaded by: [Vandenbossche, Julie]

On: 11 August 2010

Access details: Access Details: [subscription number 925549336]

Publisher Taylor & Francis

Informa Ltd Registered in England and Wales Registered Number: 1072954 Registered office: Mortimer House, 37-41 Mortimer Street, London W1T 3JH, UK



International Journal of Pavement Engineering

Publication details, including instructions for authors and subscription information:

<http://www.informaworld.com/smpp/title~content=t713646742>

Comparison of measured vs. predicted performance of jointed plain concrete pavements using the Mechanistic-Empirical Pavement Design Guideline

J. M. Vandenbossche^a; F. Mu^a; T. R. Burnham^b

^a Department of Civil and Environmental Engineering, University of Pittsburgh, Pittsburgh, PA, USA ^b Minnesota Department of Transportation, Maplewood, MN, USA

First published on: 10 August 2010

To cite this Article Vandenbossche, J. M. , Mu, F. and Burnham, T. R.(2010) 'Comparison of measured vs. predicted performance of jointed plain concrete pavements using the Mechanistic-Empirical Pavement Design Guideline', International Journal of Pavement Engineering,, First published on: 10 August 2010 (iFirst)

To link to this Article: DOI: 10.1080/10298436.2010.506536

URL: <http://dx.doi.org/10.1080/10298436.2010.506536>

PLEASE SCROLL DOWN FOR ARTICLE

Full terms and conditions of use: <http://www.informaworld.com/terms-and-conditions-of-access.pdf>

This article may be used for research, teaching and private study purposes. Any substantial or systematic reproduction, re-distribution, re-selling, loan or sub-licensing, systematic supply or distribution in any form to anyone is expressly forbidden.

The publisher does not give any warranty express or implied or make any representation that the contents will be complete or accurate or up to date. The accuracy of any instructions, formulae and drug doses should be independently verified with primary sources. The publisher shall not be liable for any loss, actions, claims, proceedings, demand or costs or damages whatsoever or howsoever caused arising directly or indirectly in connection with or arising out of the use of this material.

Comparison of measured vs. predicted performance of jointed plain concrete pavements using the Mechanistic–Empirical Pavement Design Guideline

J.M. Vandenbossche^{a*}, F. Mu^a and T.R. Burnham^b

^aDepartment of Civil and Environmental Engineering, University of Pittsburgh, Pittsburgh, PA, USA; ^bMinnesota Department of Transportation, Maplewood, MN, USA

(Received 19 January 2009; final version received 2 July 2010)

This research evaluates the ability of the Mechanistic–Empirical Pavement Design Guide (MEPDG) to accurately predict the performance of jointed plain concrete pavements (JPCPs). This is accomplished by comparing predicted performances with observed performances for the in-service mainline test cells at Mn/ROAD. These comparisons indicate that MEPDG performance predictions for JPCP are most accurate when the default (constant) built-in equivalent temperature difference of -5.5°C is used instead of a site-dependent value. It appears that significant portions of the error of estimation can be explained by the sensitivity of the performance models to variability in hardened concrete properties (modulus of rupture, modulus of elasticity and coefficient of thermal expansion) and pavement structural features (slab thickness, joint spacing, subbase type and bond condition). Predictions of slab cracking were found to be highly sensitive to these parameters. In addition, the MEPDG cracking model seemed not to fit local cracking observations for the Minnesota test cells. New calibration factors are needed to more accurately predict Minnesota JPCP slab cracking. This study also included comparisons of predicted service lives for the Mn/ROAD test cells using different design methodologies and as-built input parameters. In most cases considered, the MEPDG predicted longer service lives than did the 1993 AASHTO procedure. The MEPDG also predicted longer service lives than the PCA procedure for the 5-year cells but shorter service lives for the 10-year cells. This infers that, when holding service life constant, the MEPDG generally results in thinner concrete pavement sections than the 1993 AASHTO procedure.

Keywords: MEPDG; built-in temperature difference; jointed plain concrete pavement; cracking; service life; performance prediction

Impetus

When a new pavement design procedure is introduced, it is important to identify the inputs that significantly influence the design procedure outputs, and it is equally important to evaluate the ability of the design procedure to accurately predict pavement performance. The objective of this research was to evaluate the ability of the Mechanistic–Empirical Pavement Design Guide (MEPDG) (ARA, Inc. 2004) ver. 1.0 to predict the performance of jointed plain concrete pavements (JPCPs). This was accomplished by comparing predicted pavement performance with actual performance measures for several in-service pavements. A close look was then taken at the factors that might result in the difference between the predicted and observed performances, i.e. variation of concrete material properties and pavement structure design details. The cracking prediction model was also evaluated for local Minnesota conditions.

The evaluation process for any new design procedure should also include comparisons of designs developed using current procedures with those obtained using the new procedure. This was also accomplished under this study.

Introduction

The MEPDG is a recently developed analysis and design tool that considers factors representing all of the design inputs considered in the American Association of State Highway Transportation Officials (AASHTO) 1993 pavement design procedure. It also attempts to account, in a very comprehensive manner, for some of the key mechanisms that are known to affect pavement performance. The outputs of the new procedure include the predicted quantities of distress (i.e. cracking, spalling and faulting) and ride quality (i.e. International Roughness Index, IRI) for JPCPs present at any given time.

One of the most important improvements in the new procedure is the direct consideration of climatic effects (e.g. the development of temperature and moisture gradients in concrete paving slabs and their effects on pavement stresses and deformations), which are modelled using the Enhanced Integrated Climatic Model (EICM), which has been incorporated in the MEPDG. The EICM is capable of predicting temperature conditions through the depth of the pavement structure (i.e. it is a one-dimensional model) on an hourly basis.

*Corresponding author. Email: jmv7@pitt.edu

The mechanistic response of the pavement structure to the interaction between traffic [which is considered using actual axle load spectra as opposed to equivalent single axle loads (ESALs)] and environmental loads in the context of the material and structural properties of the pavement is managed by a neural network (NN) that is based on ISLAB2000 finite element method analyses (Khazanovich *et al.* 2001) and is incorporated in the MEPDG. By coupling the NN and the EICM, the MEPDG is able to analyse the performance of pavements on an incremental basis, taking into account the date of construction, design life and the time-based evolution of various distresses, so that the damage caused by each load can be determined in consideration of the temperature and moisture gradients present in the slab at the time of loading.

In the MEPDG models, transverse cracking is expected to occur due to fatigue. The total cracking (per cent slabs cracked) is obtained by adding predicted bottom-up and top-down cracking rates and subtracting the probability that both occur in the same slab. Bottom-up transverse cracking can occur when there exists a high positive temperature gradient through the slab (i.e. the top of the slab is warmer than the bottom of the slab). Under this condition, repeated applications of heavy axle loads result in fatigue damage at the bottom of the slab, with the greatest damage typically being done near the slab edge closest to the applied loads. For top-down transverse cracking, the fatigue damage initiates at the top of the slab due to the presence of a negative temperature gradient (i.e. the top of the slab is cooler than the bottom of the slab) and repeated heavy axle loads acting simultaneously on both ends of the slab.

Another primary distress model in the MEPDG describes the mechanism of joint faulting. Contributing factors include: repeated truck axles crossing transverse joints, poor joint load transfer efficiency (LTE) and the presence of fines and free moisture under the joint. LTE is provided by aggregate interlock along the joint, as well as the support of the base and the shoulder. It can be greatly improved by the use of mechanical devices (e.g. tie bars and dowel bars).

Ever since the birth of MEDPG, sensitivity analyses have been carried out to determine the reasonableness of its built-in models as well as the relative importance or impact of each design input (Hall and Beam 2004, Barenberg *et al.* 2005, Coree 2005, Kannekanti and Harvey 2005, Gutierrez 2008, Khazanovich *et al.* 2008). For example, Gutierrez (2008) identified that the built-in equivalent temperature difference and the Portland cement concrete (PCC) modulus of rupture were the most influential inputs for MEPDG faulting and cracking models, respectively. Other researchers have concluded that the presence of dowels and the joint spacing are critical (Kannekanti and Harvey 2005). The conclusions

of these studies are largely a function of the types of statistical analysis used to identify the critical inputs, as well as the ranges of inputs considered in the analyses.

The MEPDG can be used to predict transverse cracking (per cent cracked slabs), faulting, LTE and ride quality (IRI) for JPCP. The predictive capability of the MEDPG with regard to each of these distresses is evaluated. To accomplish this, nine JPCP sections at the Minnesota Road Research Facility (Mn/ROAD) were used to compare measured performance vs. that predicted using the MEPDG. The use of the pavement sections (test cells) constructed at Mn/ROAD is ideal in that accurate as-built construction, material characterisation and traffic data are available, along with climate data from an on-site weather station. Extensive pavement performance data are also available for a 15-year time period.

Temperature and moisture gradients can be present at the time a concrete slab sets up. Theoretically, a hardened, in-service PCC slab is flat when the transient equivalent temperature difference between the top and bottom of the slab is equal to the built-in equivalent temperature difference. Another unique aspect of the Mn/ROAD test cells is that the built-in equivalent temperature differences between the tops and bottoms of the slabs were established for each test cell in a previous study (Vandenbossche 2003). These values are referred to as being 'equivalent' temperature differences because, even though the actual temperature and moisture gradients can be highly nonlinear, the nonlinear gradients can be equated to an equivalent linear gradient by identifying the temperature difference or linear gradient that produces the same deflection basin (Janssen and Snyder 2000). Several approaches for determining the built-in equivalent temperature gradient are reported in the literature (Byrum 2000, Beckemeyer *et al.* 2002, Khazanovich and Yu 2005, Rao and Roesler 2005, Well *et al.* 2006).

It should be noted that the MEPDG built-in equivalent temperature gradient accounts for the variation in the temperature and moisture gradients in the slab at the time the slab sets up as well as for the irreversible part of concrete shrinkage over time, concrete creep and settlement of the base and subgrade (Yu *et al.* 1998, Khazanovich *et al.* 2001, Gotlif *et al.* 2006). Since there was no formal procedure for back-calculating site-specific values for this parameter at the time of the MEPDG development, it was estimated on a global basis during the MEPDG calibration. The built-in equivalent temperature gradient, $\Delta T_{\text{built-in}}$, was assumed to be the same for all sections and the default value recommended for the users in future pavement designs was selected as the value that minimised distress prediction errors (-5.5°C). Earlier studies have shown this variable to be critical to MEPDG pavement performance predictions (Hall and Beam 2004, Barenberg *et al.* 2005, Coree 2005, Kannekanti and Harvey 2005, Gutierrez 2008, Khazanovich *et al.* 2008).

Table 1. Design of Mn/DOT test sections used for analysis.

Test section	Cell	Slab thickness (mm)	Joint spacing (m)	Lane widths, inside/outside (m)	Dowel diameter (mm)	Base/subbase
5-Year	5	190	6.1	4.0/4.3	25	80 mm cl4sp over 685 mm cl3sp
	6	185	4.6	4.0/4.3	25	130 mm cl4sp
	7	195	6.1	4.0/4.3	25	100 mm PASB over 80 mm cl4sp
	8	190	4.6	4.0/4.0/4.3	25	100 mm PASB over 80 mm cl4sp
	9	195	4.6	4.0/4.0/4.3	25	100 mm PASB over 80 mm cl4sp
10-Year	10	255	6.1	3.7/3.7	32	100 mm PASB over 80 mm cl4sp
	11	240	7.3	3.7/3.7	32	130 mm cl5sp
	12	255	4.6	3.7/3.7	32	130 mm cl5sp
	13	250	6.1	3.7/3.7	38	130 mm cl5sp

Therefore, it is important to determine whether the magnitude of the site-specific value of $\Delta T_{\text{built-in}}$ can be used as an input in the MEPDG.

Description of Mn/ROAD test cells

Mn/ROAD is a densely instrumented pavement test facility constructed adjacent to Interstate Route 94 (I-94) approximately 65 km northwest of Minneapolis, Minnesota. This study used performance data collected from the nine test cells that constitute the 5- and 10-year mainline concrete pavement test sections, which represent different combinations of slab thickness, joint spacing, restraint conditions and subbase types. The slab thicknesses of the 5- and 10-year cells were designed to be 190 and 240 mm, respectively. The length of each cell is approximately 150 m and all test sections have asphalt shoulders. The test cells are loaded by live service traffic that has been diverted from the regular westbound lanes of I-94. The annual average daily traffic (AADT) is currently (in 2009) about 24,000 vehicles per day with about 12% heavy truck traffic. The ESALs accumulated so far are approximately 20 million since the construction of these sections in 1994.

Table 1 presents the basic design characteristics of the Mn/ROAD test cells. Table 2 shows the measured properties of the hardened PCC used in these test cells, and Table 3 provides the aggregate gradation specifications for the granular base and subbase layers used in these test cells (as provided by the 1995 Minnesota Department of Transportation (Mn/DOT) Specification Standards).

The built-in equivalent temperature differences ($\Delta T_{\text{built-in}}$) for the Mn/ROAD pavement cells are known to be equal to zero. The actual values of $\Delta T_{\text{built-in}}$ for these test cells are significantly different from the default (constant) MEPDG value of -5.5°C that was assigned to all sites used in the cracking regression model implemented in the MEPDG. This provides an opportunity to evaluate performance predictions at $\Delta T_{\text{built-in}}$ values other than -5.5°C and compare them to the predictions developed when using $\Delta T_{\text{built-in}} = -5.5^{\circ}\text{C}$.

Evaluating cracking prediction

The MEPDG was used to predict transverse cracking for each of the 5- and 10-year mainline test cells at Mn/ROAD at a level of reliability of 50%. A summary of the predicted

Table 2. Concrete properties of Mn/ROAD cells.

Test section	Cell	M_r , modulus of rupture (28-day) (MPa)	E_C , modulus of elasticity (28-day) (MPa)	CTE ($10^{-6}/^{\circ}\text{C}$)	$\Delta T_{\text{built-in}}$, permanent curl/warp effective temperature difference ($^{\circ}\text{C}$)
5-Year	5	4.3	25,500	8.1	-0.1
	6	3.9	31,500	8.1	0
	7	4	27,000	8.1	0
	8	3.5	31,000	8.4	0
	9	3.9	29,500	9.8	0
10-Year	10	4.3	21,500	8.1	0
	11	5	26,000	6.7	0
	12	4.6	28,500	8.8	0
	13	4.7	27,500	8.8	0

Table 3. Mn/DOT 1995 granular specifications (per cent passing).

Sieve size	Base material			
	cl3sp	cl4sp	cl5sp	PASB
38.1 mm	–	100	–	–
31.75 mm	–	–	–	100
25.4 mm	–	95–100	100	95–100
19.05 mm	–	90–100	90–100	85–98
12.7 mm	100	–	–	–
9.525 mm	95–100	80–95	70–85	50–80
No. 4	85–100	70–85	55–70	20–50
No. 10	65–90	55–70	35–55	0–20
No. 20	–	–	–	0–8
No. 40	30–50	15–30	15–30	0–5
No. 200	8–15	5–10	3–8	0–3

Notes: Special crushing requirements (sp); cl3sp and cl4sp: crushed/fractured particles are not allowed; cl5sp: 10–15% crushed/fractured particles are required; PASB, permeable asphalt stabilised base.

cracking for each of these runs is provided in Table 4. A best-fit analysis between the predictions and the observations is also carried out, as summarised in Table 4, where the slope implies the ratio of the mean observation to the mean prediction and the R^2 indicates how well the variance of the predictions fit the variance of the performance.

The first MEPDG run was made using the measured values for $\Delta T_{\text{built-in}}$ and as-built material properties and environmental conditions. Table 4 shows that the resulting predictions of slab cracking are extremely different from actual observed rates of cracking for all cells except Cells 10 and 12. It is difficult to determine why the MEPDG cracking predictions were reasonably accurate for Cells 10 and 12 but not for the other cells because Cells 10 and 12 do not share any common factor that is not represented in other cells.

Built-in temperature gradient

Another study indicated that it was best if the input value for $\Delta T_{\text{built-in}}$ was treated as a constant rather than as a variable in the MEPDG (Vandenbossche and Mu 2009). To validate these findings, a second series of MEPDG runs were made using the same inputs as the first run except using the MEPDG default value of $\Delta T_{\text{built-in}}$ (-5.5°C). The results of these analyses are summarised in Table 4, which shows that the MEPDG predictions of slab cracking improved greatly for all cells, but that they were reasonably accurate only for Cells 10–12. It can be noted that the greatest improvements in crack prediction accuracy were observed for the test sections with longer joint spacings (Cells 5, 7, 11 and 13). The prediction for Cell 9 also improved greatly, even though it has a shorter panel length. The results of these analyses suggest that it may be beneficial to use the default value for $\Delta T_{\text{built-in}}$

Table 4. MEPDG cracking analysis for Mn/ROAD mainline pavement test cells.

Cell	5	6	7	8	9	10	11	12	13
Observed cracking, % slabs	15	0	0	0	0	0	9	0	0
Predicted cracking, % slabs									
Meas. built-in ^a and as-built conditions ^a (%)	100	100	96	99	92	0	58	3	98
Default built-in ^b and as-built conditions ^a (%)	65	100	25	83	28	0	1	0	19
Default built-in ^b , $M_r = 4.3 \text{ MPa}$, $E_c = 27,600 \text{ MPa}$ and $\text{CTE} = 8.1 \times 10^{-6} / ^\circ\text{C}$ (%)	84	89	9	1	1	0	86	0	48
Default built-in ^b , $M_r = 4.7 \text{ MPa}$, $E_c = 29,200 \text{ MPa}$ and $\text{CTE} = 8.1 \times 10^{-6} / ^\circ\text{C}$ (%)	65	74	4	1	0	0	67	0	20

^a See Table 2.

^b -5.5°C .

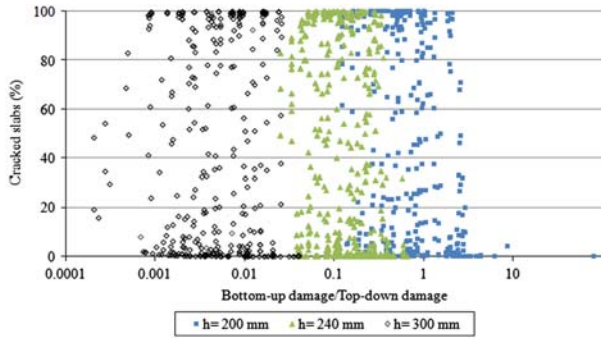


Figure 1. Predicted JPCP slab cracking as a function of the ratio of bottom-up damage to top-down damage for various slab thicknesses.

in MEPDG predictions even when the actual value can be determined. The work performed by Gutierrez (2008) supports this recommendation.

The fact that decreasing $\Delta T_{\text{built-in}}$ from a measured value of about zero to the default value (-5.5°C) decreased the predicted cracking suggests that the predicted failure mode is bottom-up fatigue damage when the measured values are used. When the default built-in temperature difference is used, it appears that thicker pavements are predicted to develop more top-down cracking, as shown in Figure 1, which summarises results obtained from some of more than 3000 MEPDG runs that are part of a sensitivity analysis performed under a study for the Federal Highway Administration (Vandenbossche *et al.* 2008). Historically, it has been assumed that pavements fail from cracks initiating at the bottom of the slab. However, the results of these studies indicate that the mode of cracking predicted by the MEPDG can be driven by the selected value of the $\Delta T_{\text{built-in}}$. Based on the results of the current analysis, it seems that the role of $\Delta T_{\text{built-in}}$ in the MEPDG may be that of a calibration constant rather than that of an actual as-built property.

PCC material properties

It is important to characterise the sensitivity of performance prediction models to the levels of variability in material properties typically found in construction. This section focuses on the effects of variability in measured concrete material properties on predicted cracking. The three concrete material properties that were measured for the concrete used to pave the Mn/ROAD test cells were flexural strength (M_r), elastic (Young's) modulus (E_c) and coefficient of thermal expansion (CTE)/contraction.

The same PCC mixture design and concrete aggregate source were used to construct all of the test sections. The average 28-day M_r was 4.3 MPa, with a standard deviation (SD) of 0.4 MPa, resulting in a coefficient of variation of 10.4%. Variability in the measured strengths

can be attributed to many sources, including normal variability in the properties of the mixture components, possible segregation during the construction process, and techniques used during the preparation and testing of the specimens. It was assumed for this study that the average value of all of the measured strengths is representative of the average strength of the concrete throughout each section; this value (4.3 MPa) was used as a starting point in predicting estimated cracking using the MEPDG.

The E_c was 27,600 MPa with a SD of 2900 MPa and a coefficient of variation of 10.5%. The overall average value of E_c (27,600 MPa) was selected for use as a starting point in predicting cracking in the Mn/ROAD cells using the MEPDG.

It is interesting to note that the relationship between M_r and E_c varies between the cells. For example, cells with higher M_r values often present lower E_c values. This illustrates the variability of measured material properties (especially in those that should be linked) and emphasises the need to understand the sensitivity of test results to such known variability.

The average CTE for all the cells was $8.3 \times 10^{-6}/^{\circ}\text{C}$; the median value was $8.1 \times 10^{-6}/^{\circ}\text{C}$. The SD was $0.8 \times 10^{-6}/^{\circ}\text{C}$, producing a coefficient of variation of 9.4%. The variability is slightly larger than what would generally be anticipated for the same mix for within-lab testing but would be good for between-lab results. Forensic evaluations of some cores from the test cells showed large amounts of segregation. The cores also showed that the total volume of aggregate present appeared to vary between cores. The CTE of the concrete can be estimated by using the weighted average of the constituent (i.e. aggregate and paste) based on the relative volumes of the constituent (Packard and Tayabji 1985). Based on this, changing the concrete aggregate content by $\pm 10\%$ can result in changes in the CTE of $\pm 2 \times 10^{-6}/^{\circ}\text{C}$ for the type of aggregate used in this project. These factors all help to explain the observed variation in the measured CTE when the same concrete mixture design was used to construct all of the cells. It also helps explain why the CTE of $6.7 \times 10^{-6}/^{\circ}\text{C}$ measured for the core pulled from Cell 11 might not be representative of the cell as a whole. It is believed that $8.1 \times 10^{-6}/^{\circ}\text{C}$ best represents the average CTE for all cells since this value is the median and was the average obtained for four of the nine cells.

The MEPDG was used to predict the slab cracking for each cell using the average M_r and E_c and the median CTE of all cells; the results are provided in Table 4. There was a significant improvement in the accuracy of the cracking predictions for Cells 7–9, as is also indicated by a greater slope and a larger R^2 in Table 5.

It is interesting to note that the predicted slab cracking measures for Cells 8 and 9 are substantially different (83% cracking vs. 28% cracking) when the measured PCC material properties of each cell were used, even though the

Table 5. Best fit between predictions and observations for the cases defined in Table 4.

	Slope of the linear best fit between observations and predictions	R^2 of the linear best fit between observations and predictions
Meas. built-in ^a and as-built conditions ^a	0.03	0.02
Default built-in ^b and as-built conditions ^a	0.04	0.01
Default built-in ^b , $M_r = 4.3$ MPa, $E_C = 27,600$ MPa and CTE = $8.1 \times 10^{-6}/^\circ\text{C}$	0.08	0.43
Default built-in ^b , $M_r = 4.7$ MPa, $E_C = 29,200$ MPa and CTE = $8.1 \times 10^{-6}/^\circ\text{C}$	0.11	0.44

^a See Table 2.^b -5.5°C .

structural designs for these two cells are very similar. This difference in predicted cracking can be attributed to the differences in measured M_r and E_C values for these individual cells (i.e. Cell 9 cores exhibited higher average M_r and lower E_C values when compared to Cell 8). When overall average M_r and E_C values were used, the predicted cracking was 1% for both cells.

Conversely, the cracking predictions for Cells 5, 11 and 13 became less accurate when the project average M_r and E_C values were used as inputs (rather than cell-specific values). For these cells, the M_r measured for each cell was higher than the project average M_r . Using the (lower) average M_r as an input resulted in a significant increase in the predicted cracking, even though little to no cracking has been observed in these cells. In addition, the CTE measured for Cell 11 was much lower than the median value determined for all cells, so using the median (higher) CTE value for this cell also contributed to the resulting increase in predicted cracking.

To further evaluate the effects of variability in PCC material properties on MEPDG-predicted cracking, another set of analysis runs was performed using M_r and E_C inputs that represented project average values plus one SD (i.e. $M_r = 4.7$ MPa and $E_C = 29.2$ GPa). The results of these runs are also provided in Table 4. Although this change helps to improve the accuracy of the cracking

predictions (as indicated by Table 5), predicted values are still substantially higher than observed values for several of the cells.

The results of the analyses above suggest that the main effects and interaction effects of PCC M_r , E_C and CTE on predicted slab cracking are highly significant. The sensitivity of the MEPDG cracking prediction to variations in these inputs was further evaluated by performing additional runs of the MEPDG as described below. The predicted cracking of Cell 13 was determined repeatedly while systematically substituting the measured concrete properties of Cell 11 for those of Cell 13 in a full factorial experimental design pattern, as shown in Table 6. The seven substitution cases considered are labelled A through G.

The predicted percentages of slab cracking for cases A through G are shown, along with observed cracking data, in Figure 2. This figure shows that the MEPDG cracking prediction for case G (which uses M_r , E_C and CTE properties from Cell 11) most closely matches the observed cracking data.

The last column in Table 6 summarises the predicted slab cracking for each case after 15 years of service. Table 6 and Figure 2 show that changing each of the concrete strength input parameters individually (i.e. cases A, B and D) did not result in accurate predictions of

Table 6. Predicted cracking for Cell 13 for cases replacing PCC properties in Cell 13 with those measured for Cell 11.

Case	E_C (MPa)	M_r (MPa)	CTE ($10^{-6}/^\circ\text{C}$)	Observed cracking in year 15 (% slabs cracked)	Predicted cracking in year 15 (% slabs cracked)
Base	27,500	4.7	8.8		19.0
A	26,000	4.7	8.8		16.3
B	27,500	5	8.8		7.7
C	26,000	5	8.8		4.2
D	27,500	4.7	6.7	0.0	2.2
E	26,000	4.7	6.7		0.8
F	27,500	5	6.7		0.3
G	26,000	5	6.7		0.2

Note: Italicised values correspond to replaced values.

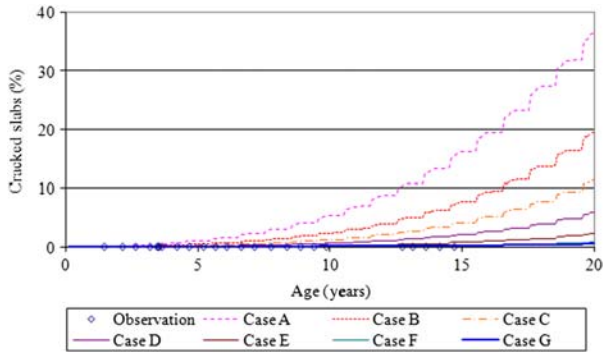


Figure 2. Prediction of slab cracking of Cell 13 for various PCC property inputs.

observed slab cracking; they also show that the interaction of all three of these factors contributed to the convergence of predicted and observed slab cracking, with cases F and G producing the most accurate predictions. It can also be noted that changing the CTE produced the greatest changes in the predicted rates of cracking while changing the M_r produced the smallest changes.

Further insight into the sensitivity of the predicted cracking to variations in properties of the hardened PCC can be obtained by looking at the relationship between per cent cracking and damage that is used in the MEPDG, which is depicted in Figure 3. This figure shows that small changes in damage can significantly increase or decrease slab cracking if the accumulated damage is in ‘the critical zone’ (i.e. accumulated fatigue damage between about 0.1 and 1). The total amount of damage can be shifted to the left of the critical zone, where the effects of small changes in accumulated damage do not produce such significant changes in slab cracking. This can be accomplished to varying degrees by many means, including: (1) by decreasing E_C (which reduces slab stresses), (2) by increasing M_r (which decreases the stress ratio for any

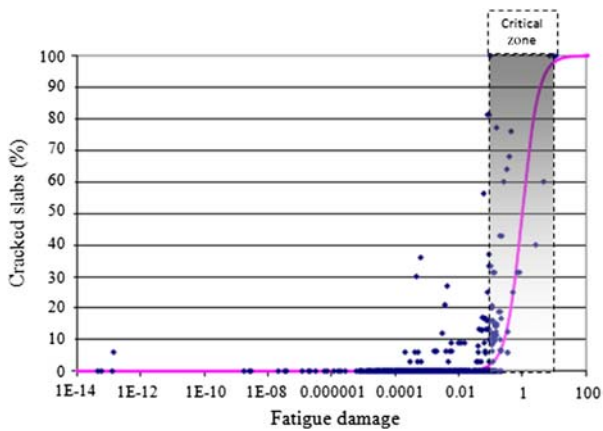


Figure 3. Fatigue damage-slab cracking model used in the MEPDG.

applied stress), (3) by decreasing CTE (which reduces curl/warp-related stresses), (4) by increasing slab thickness (which decreases load-related stresses), (5) by other design and materials modifications, and (6) by any combination of the above. The individual and combined effects of varying the first three factors are illustrated in Table 6 and Figure 2, which show just how drastically the predicted slab cracking can change (and can be from the observed slab cracking) with just a few small differences between the designed pavement parameters and the as-built parameters.

Calibration of transfer function

Further insight into the sensitivity of the predicted slab cracking model to variations in the PCC properties can be obtained by reconsidering the MEPDG relationship between accumulated fatigue damage and slab cracking, which is shown in Figure 3. This fatigue damage-cracking performance curve was calibrated during the MEPDG development using data from 516 observations obtained from nearly 200 JPCP sections located throughout the USA. In spite of this broad calibration database, the national calibrated curve does not seem to fit data from the Mn/ROAD test cells, which seem to consistently outperform the predictions of the MEPDG-cracking model at Mn/ROAD, as indicated by Figure 4. Considered another way, the Mn/ROAD-cracking data points would be plotted to the right of the performance curve presented in Figure 4, while nearly all the calibration data lie on the left side of the curve. This suggests that new calibration factors should be established for this model to provide a better fit for Minnesota applications of the model.

The cracking prediction equation, established using the previously described national performance data (1), is given as

$$\text{Cracking} = \frac{100}{1 + C4 \text{Fatigue}^{C5}}, \quad (1)$$

where $C4 = 1$ and $C5 = -1.98$. The R^2 for this model is 0.75.

Based on the performance data currently available from the Mn/ROAD test cells, the local calibration coefficients for the Mn/ROAD sites would be $C4 = 10^5$ and $C5 = -10$. The R^2 of the fitted curve is quite low (i.e. less than 0.1), in part due to the lack of cracking observed to date and because of the limited number of test sites and available data. The Mn/ROAD test sections should be of great value in performing a local calibration after more distress has developed in these sections; further development of the local calibration coefficients should be pursued at that time.

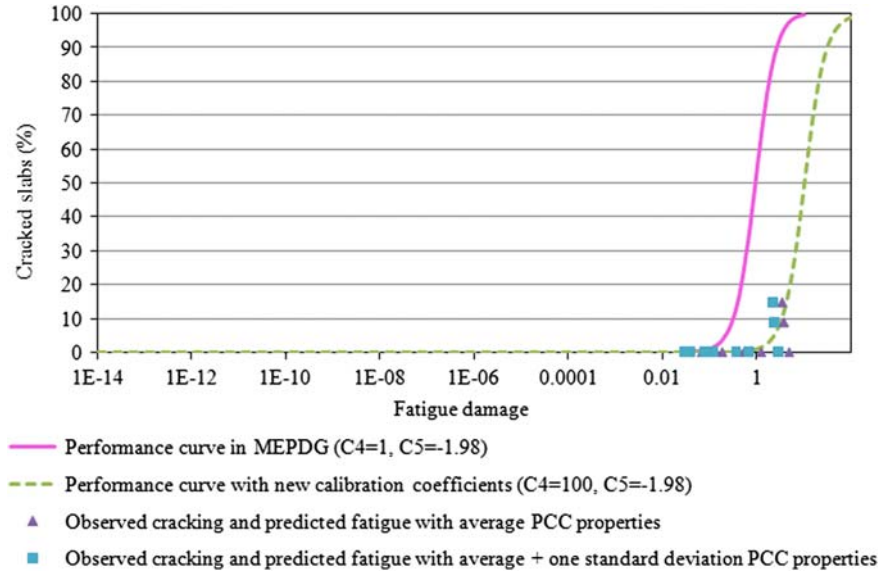


Figure 4. MEPDG performance curve vs. locally calibrated performance curve.

Pavement structure

The accuracy of the MEPDG-predicted slab cracking was evaluated with respect to the structural parameters of the pavement being analysed. One observation that has been made is that it appears the MEPDG tends to overpredict transverse cracking more frequently when a granular base is used than when stabilised bases are used (Vandenbossche *et al.* 2008). Additional runs of the MEPDG were performed to further evaluate the sensitivity of the MEPDG to the range of slab thicknesses, subbase types and joint spacings represented in the 5- and 10-year mainline cells at Mn/ROAD. Each run was performed using identical PCC material properties ($M_r = 4.3$ MPa; $E_C = 27,600$ MPa and $CTE = 8.1 \times 10^{-6}/^{\circ}C$) in order to isolate the effects of the changes in the structural parameters on predicted cracking.

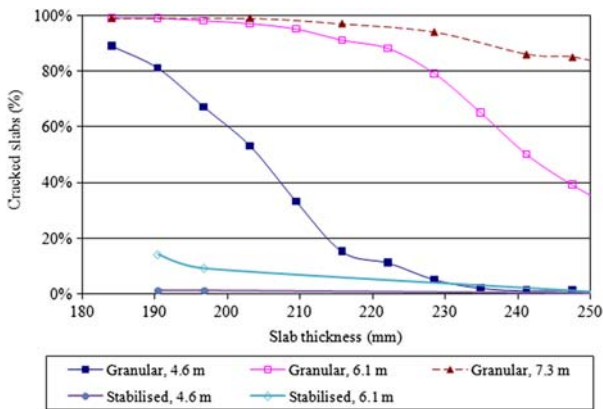


Figure 5. Sensitivity of predicted JPCP slab cracking to slab thickness, subbase type and joint spacing.

The results of these runs are shown in Figure 5, which shows that increases in predicted cracking with increasing joint spacing (for a given pavement thickness) are significantly smaller for the stabilised subbase cases than for the unstabilised subbase cases. It can also be seen that the predicted rates of slab cracking are generally much lower for the unstabilised subbase cases than for the stabilised subbase cases. This is reflected in the high cracking rates predicted for Cells 5 and 6 compared to those predicted for Cells 7–9, as shown in Table 4. A similar trend can be seen for the 10-year cells (Cell 10 vs. Cells 11–13).

Similar results were found in sensitivity analyses performed for the FHWA. Predicted cracking rates were determined for two different types of subbase (open-graded asphalt-stabilised vs. granular). Data from more than 3000 MEPDG runs indicate that more than 50% of the pavements modelled with asphalt-treated subbases were predicted to exhibit less than 10% cracking, while 50% of the slabs modelled with granular subbases were predicted to exhibit more than 70% cracking (Mu *et al.* 2010).

These trends are counter-intuitive and anomalous. Stabilised subbases are typically used because they help to reduce the potential for faulting. However, stabilised subbases generally deform less than granular subbase materials, resulting in larger unsupported slab areas and correspondingly higher curling/warping stresses in the presence of temperature and moisture gradients, resulting in increased potential for slab cracking.

Consideration of the assumed bond condition between the slab and stabilised subbase might help to explain this anomalous performance prediction. If the stabilised subbase remains bonded to the bottom of the slab, the

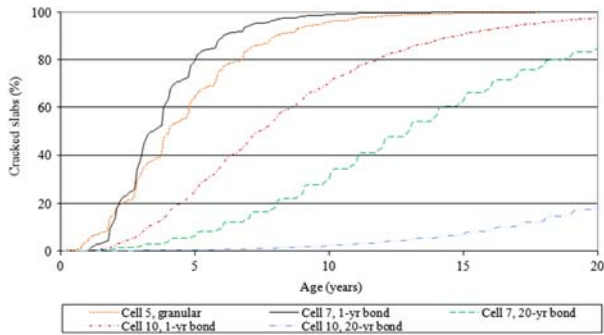


Figure 6. Effects of subbase type and slab–subbase bond condition on cracking for selected Mn/ROAD test cell variables.

slab–subbase system will act as a composite slab with an effective stiffness that is greater than that of the slab alone. In this case, slab stresses would be reduced and a larger number of loads would be carried before slab cracking develops. This behaviour is illustrated in Figure 6, which shows the predicted slab cracking for similar pavement sections (Cell 5, 190 mm-thick PCC slab on granular subbase and Cell 7, 195 mm-thick PCC slab on asphalt-treated base) assuming three different subbase support and bonding conditions: (1) stabilised subbase with debonding assumed to occur after 1 year; (2) stabilised subbase where the bond between the slab and subbase lasts 20 years; and (3) granular (unbonded, unstabilised) subbase.

For the example presented in Figure 6 and assuming a failure criterion of 20% slab cracking, the pavement with the granular subbase (Cell 5) and with the stabilised subbase that became debonded after 1 year (Cell 7) would both fail after approximately 2 years. However, the pavement with a stabilised subbase developed less cracking in the first year when the bonding was active. The development of cracking is delayed until well after year 8 when slab–subbase bond is maintained for 20 years. It can be concluded that slab–subbase bond condition can help to explain why a pavement with a stabilised subbase might exhibit less cracking than one with a granular subbase. However, one would still expect the pavement with the granular subbase to exhibit substantially less cracking than the one with stabilised subbase that became debonded after 1 year unless the joint spacing was sufficiently short that curling/warping stresses become insignificant.

Coring at Mn/ROAD has shown that good bond still exists between the slab and the stabilised subbase (in cells using stabilised subbase materials); therefore, it was assumed that the bond lasts the life of the pavement structure when predicting cracking using the MEPDG. If the bond was assumed to fail before the end of the analysis period, the predicted cracking values (presented in Table 4) would have been even more divergent from the observed cracking values.

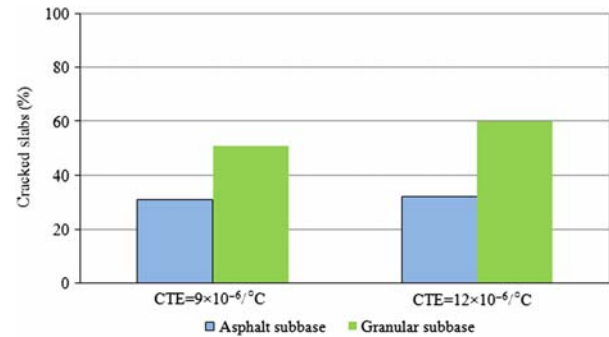


Figure 7. Effects of subbase type on JPCP slab cracking for different CTEs.

The MEPDG is quite sensitive to the assumed slab–subbase bond life, even for thicker slabs. Besides Cells 5 and 7, Figure 6 also presents the result of MEPDG runs that were made for Cell 10 (255 mm-thick PCC slab on asphalt-treated subbase). All three cells have the same panel length (6.1 m). Project average PCC material properties were used for all three cases so that predicted performance differences would be attributed solely to the effects of slab thickness, subbase type and slab–subbase bond condition. The cracking predicted for Cell 7 (thinner slab on a stabilised base) is lower than that predicted for a thin slab on a granular subbase (Cell 5) as long as the slab and stabilised base are bonded. When slab–stabilised subbase bond is assumed to fail after 1 year, the predicted cracking of Cell 7 soon surpasses that of Cell 5. Comparing the cracking prediction curves for 1-year bond life and 20-year bond life assumptions for both Cells 7 and 10, it can be seen that the effect of the slab–subbase bond condition appears to be more significant for thicker slabs.

This behaviour can be further evaluated by examining the sensitivity of the predicted slab cracking to subbase type and varying CTE properties. Figure 7 summarises the results of data from the previously referenced 3000-run FHWA study of MEPDG sensitivity (Vandenbossche *et al.* 2008) and shows that increasing the concrete CTE (by 33%) strongly affects slab cracking in the cases with granular subbase materials (presumably due to significantly increased curl/warp stresses) but has little effect on slab cracking for cases using stabilised subbase materials (presumably due to composite action of the bonded slab subbase).

The other observation that can be made from this analysis concerns the sensitivity of the MEPDG-predicted slab cracking to relatively small changes in slab thickness. For example, considering Figure 5 and the data provided for the pavement with the granular subbase and 4.6 m panel lengths, it can be seen that a 215 mm slab thickness would meet the performance criterion of having less than 20% predicted slab cracking throughout the pavement

service life. Decreasing the slab thickness by just 6 mm (to 209 mm) results in the prediction of about twice as much slab cracking (about 35% total) at the end of the pavement performance period. Given that it is not uncommon for PCC slab thickness to vary by ± 10 mm on many projects, it is important that designers be aware of and consider the effects of typical slab thickness variability on slab-cracking performance when establishing final design thicknesses.

Evaluating load transfer, faulting and IRI predictions

The ability of the MEPDG to accurately predict transverse joint LTE, joint faulting and IRI was evaluated.

The MEPDG generally did a good job of predicting LTE, as is shown in Figure 8, where the predicted LTE is compared to the measured values for Cell 11. Although seasonal variation in LTE was observed in both the predicted and measured LTE values, these values remained relatively constant over time. Measured seasonal LTE variations were generally slightly higher than observed LTE variations. It was also noted that the LTE does not appear to be influenced by the input value for $\Delta T_{\text{built-in}}$. These observations held true for all of the 5- and 10-year cells at Mn/ROAD.

The MEPDG also predicted the observed faulting relatively well for the Mn/ROAD test sections. To illustrate, the measured and predicted faulting values over time are provided in Figures 9 and 10 for Cells 11 and 6, respectively. The predictions were reasonable estimates of measured faulting for the first 8–10 years of pavement service life, after which time-observed faulting levels fell unexpectedly. It should be noted that the differences between predicted and observed faulting were generally well within the margin of error of faulting measurements. The faulting analyses for each cell (which, in the interest of brevity, are not all presented here) indicate that the faulting predictions developed using the default value of

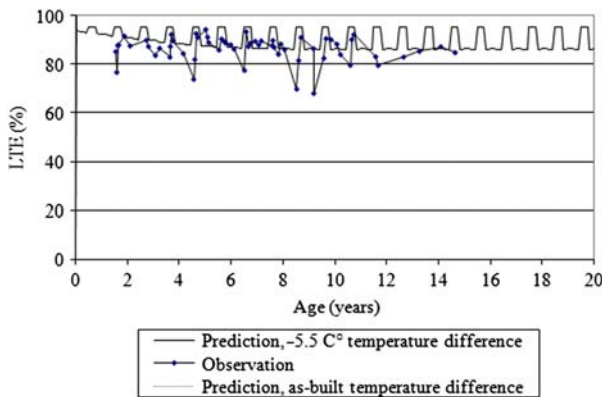


Figure 8. Predicted and observed LTE for Cell 11.

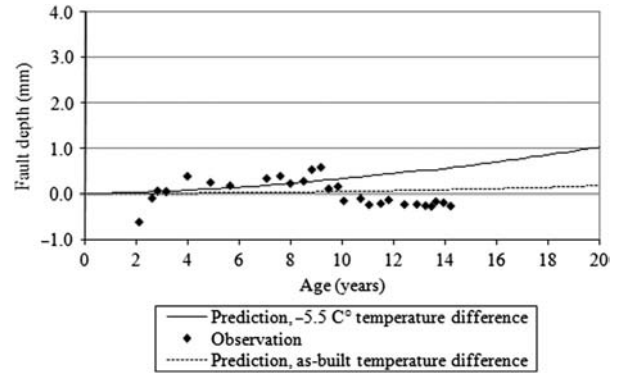


Figure 9. Predicted and observed faulting for Cell 11.

$\Delta T_{\text{built-in}}$ (i.e. -5.5°C) increase at faster rates than those of the observed faulting. The faulting predictions obtained when the default value of $\Delta T_{\text{built-in}}$ was used resulted in more accurate faulting predictions for each cell for the first 8–10 years of pavement service life, after which predictions obtained using the measured as-built values of $\Delta T_{\text{built-in}}$ were found to produce more accurate faulting predictions.

The accuracy of MEPDG IRI predictions was also evaluated. Since the MEPDG estimates of IRI are based on predicted distress values, the accuracy of the IRI prediction is directly related to the accuracy of the MEPDG slab cracking, faulting and LTE models (as well as the accuracy of the MEDPG IRI model). Recall that longer-term faulting predictions (i.e. for service life > 10 years) improved by using the measured as-built values of $\Delta T_{\text{built-in}}$ but that cracking predictions improved by using the default value of $\Delta T_{\text{built-in}}$ (see Figure 4). Predicted and observed IRI values for Cell 11 are plotted against pavement age in Figure 11, which shows that the accuracy of the IRI predictions was best when the default value of $\Delta T_{\text{built-in}}$ (-5.5°C) was used.

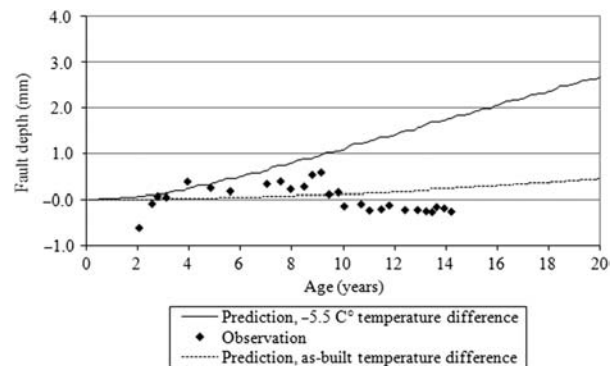


Figure 10. Predicted and observed faulting for Cell 6.

Downloaded By: [Vandebossche, Julie] At: 02:58 11 August 2010

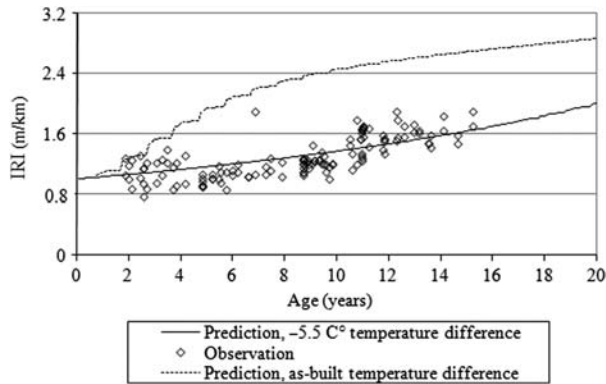


Figure 11. Predicted and observed IRI for Cell 11.

Comparison between various design methodologies

The service lives of the Mn/ROAD mainline PCC test sections were predicted using the MEPDG and compared to predictions obtained using several other design methods. A previous study evaluated three separate methods for predicting design life (Burnham and Pirkl 1997). These methods included the 1993 AASHTO Guide for Design of Pavement Structures (using 50% reliability) and the Portland Cement Association (PCA) Design for Concrete Highway and Street Pavements (1984), which has a built-in level of reliability between 90 and 95% (Packard and Tayabji 1985).

As-built parameters for variables such as M_r , E_C and initial IRI were used in the analysis. Each additional design input (such as the k -value) was established using the methodologies defined within each respective procedure. For example, the concrete M_r was determined based on 28-day third-point loading beam tests (ASTM C 78-84) using samples obtained during construction. Detailed information on how each of the parameters was established can be found in Vandembossche *et al.* (2008). All designs were based on traffic that would produce 1 million ESALs in the first year with a compound traffic growth rate of 2.5%. The default values in the MEDPG for vehicle class distribution, axle load distribution factors and hourly and monthly distributions, which were obtained from national calibration efforts, were employed.

A detailed comparison of the predicted performances obtained using the PCA and AASHTO 1993 design procedures is provided in Vandembossche (2003); the focus here is on comparing the predicted lives obtained using these procedures with the predicted life obtained using the MEDPG.

Measured as-built PCC properties were used for all cells in this analysis. A summary of the results of the MEPDG runs for this analysis is provided in Table 7, which shows that the MEPDG predicts transverse cracking as the mode of failure for the 5-year cells. All of the 10-

Table 7. MEPDG performance predictions for Mn/ROAD mainline PCC test cells.

Cell	Predicted performance			
	Cracking ^a (%)	Fault depth ^b (mm)	IRI ^c (m/km)	Predicted life (years)
5	<i>15</i>	0.89	1.88	6
6	<i>15</i>	0.03	1.61	1
7	<i>15</i>	1.5	1.89	11
8	<i>15</i>	0.25	2.08	3
9	<i>15</i>	1.88	2.38	11
10	0.3	1.63	2.72	33
11	3.3	1.09	2.72	31
12	0.2	1.68	2.72	30
13	<i>15</i>	1.5	2.12	15

Note: Italicised values indicate distress that exceeds the threshold criteria.

^aDefault threshold criteria: 15% cracking.

^bDefault threshold criteria: 3.05 mm.

^cDefault threshold criteria: 2.72 m/km.

year cells, with the exception of Cell 13, are predicted to fail due to excessive roughness. The failure mode predicted for Cell 13 is transverse cracking.

Table 8 provides a summary of the estimated service lives for each test cell, as predicted by the various design methodologies. In general, the MEPDG typically predicts service lives for the thinner slabs (5-year mainline cells) that are as long as (or longer than) those predicted using the other design methodologies. All design methods underestimated the projected performance lives of the 5-year design test cells. The MEPDG predicts longer service lives for the thicker (10-year design) Mn/ROAD test cells than those estimated by the 1993 AASHTO procedure, but less than those estimated by the PCA procedure, even though a greater level of reliability is incorporated in the PCA procedure. When the failure mode is fatigue cracking, the MEPDG and the 1993 AASHTO procedures result in similar predicted performance lives. The predicted performances obtained using the MEPDG procedure were more similar to those obtained from the PCA procedure when the mode of failure was not fatigue cracking.

Table 8. Comparison of service-life predictions for Mn/ROAD mainline PCC cells using various design methods.

Test cells	1993 AASHTO (50% reliability)	1984 PCA method	MEPDG
5	5	3	6
6	3	1	1
7	9	2	11
8	3	1	3
9	7	2	11
10	19	76	33
11	12	60	31
12	16	76	30
13	16	69	15

For most of the designs considered (and holding projected performance life constant), the MEPDG would result in thinner slab design thicknesses when compared to designs obtained using the 1993 AASHTO procedure. Using the MEPDG would also result in thinner slabs for the 5-year cells than does the PCA procedure, but thicker designs for the 10-year cells.

Summary and conclusions

When a new design procedure is introduced, it is important to evaluate its ability to predict actual pavement performance. In this research, a validation of MEPDG is carried out in terms of its ability to predict the performance of JPCPs. This is accomplished by comparing the predicted and observed performance parameters of several in-service mainline test cells at Mn/ROAD, which is a densely instrumented pavement test facility that was not used in the calibration of MEPDG. Comparisons between observed and predicted slab cracking values indicate that it is best if the $\Delta T_{\text{built-in}}$ is treated as a constant (using the MEPDG-recommended default value) rather than as a site-specific input variable in the MEPDG analysis. Furthermore, when the default value of $\Delta T_{\text{built-in}}$ is used in the MEPDG analysis, concrete pavements tend to fail due to top-down cracking most of the time.

A close look was taken at the impacts of the PCC material properties, pavement structural parameters and the MEPDG standard fatigue damage-cracking performance curve on MEPDG predictions of slab cracking. It was noted that, even though the same PCC mixture design was used for all the cells, there was significant variability in the results of tests of as-built PCC properties between cells. Cracking performance predictions were greatly improved by using PCC property inputs that represented the average and/or median of all measurements in all test cells; these values are believed to be more representative of the true values of properties in each cell. A sensitivity analysis of the effects of M_r , E_C and CTE suggests that small changes in input values for these properties can lead to significant changes in predicted performance.

The effects of pavement structural features (e.g. slab thickness, joint spacing, subbase type and slab–subbase bond condition) on slab-cracking predictions were investigated. It was found that, in some cases, a decrease in slab thickness for the studied pavement of as little as 6 mm would result in premature failure. This illustrates the need to be aware of the potential differences between the designed pavement and as-built pavement sections when establishing the final design thickness, because variations in slab thickness of ± 10 mm are not uncommon in construction.

An apparent performance prediction anomaly was also found: the use of a stabilised subbase is predicted to reduce transverse slab cracking while the use of an unbound

(granular) subbase is predicted to result in higher rates of cracking. This may be explained by consideration of the slab–subbase bond condition. The significance of the bond on the predicted cracking has been clearly illustrated in this study. However, there is no guidance provided within the MEPDG in how to determine the degree of bond or how long the bond would be effective. It would be beneficial if such guidance is established. Another apparent anomaly is that the increase in predicted cracking with increasing joint spacing is significantly larger for the pavements with unstabilised subbases than for those with stabilised subbases.

It was also concluded that the MEPDG fatigue damage-slab cracking performance curve that was calibrated nationally does not necessarily fit local performance data. For example, it tends to overestimate the predicted cracking for the Mn/ROAD facility. To improve the predictability, there is a need to establish local calibration factors for such cases.

One of the disadvantages of the MEPDG is that it takes into account the reliability based on the assessment of the overall standard error of predicted distresses as compared to the observed distresses. Since mean values for the inputs were used in establishing the reliability levels, the variance of the inputs is not associated with the predictions. This study shows that the MEPDG presents the highest predictability in both mean values and variance if the mean value of the material input is used and furthermore it seems extremely sensitive to the inputs, even within their normal variance.

The MEPDG did a good job in predicting the observed levels of LTE and faulting. Even though seasonal variations in both predicted and observed LTE values were noted, overall LTE measures for each test cell remained relatively constant over time. The faulting prediction obtained when the default value of $\Delta T_{\text{built-in}}$ was used more closely matched the observed performance for each cell. A better prediction of the observed IRI was also achieved when the default $\Delta T_{\text{built-in}}$ of -5.5°C was used.

The evaluation process for any new design procedure should also compare designs achieved using current procedures with those obtained using the new procedure. Therefore, a comparison was made between the predicted service lives of the Mn/ROAD test cells as determined using the MEPDG and other design methods. It was found that, in general, the MEPDG typically predicts service lives for thinner slabs (i.e. the Mn/ROAD 5-year test cells) that are as long as (or longer than) those developed using other design procedures, and that all of the considered design procedures underestimated the projected performance lives of these cells. For the thicker slabs (i.e. the Mn/ROAD 10-year test cells), the MEPDG predicts longer service lives than those estimated by the 1993 AASHTO procedure, but shorter lives than those estimated by the PCA procedure, even though a higher level of reliability

is incorporated in the PCA procedure. For most designs considered, the MEPDG would result in thinner slabs than would be obtained using the 1993 AASHTO procedures (holding service life constant). Using the MEDPG would also result in thinner designs than the PCA procedure for the 5-year cells, but thicker designs for the 10-year cells. Although the MEPDG seems to overpredict transverse cracking, thereby providing an overly conservative design, it still provides an adequate, if not an improved, estimate of the predicted service life when compared to the PCA and 1993 AASHTO procedures.

Acknowledgements

The authors would like to gratefully acknowledge the Federal Highway Administration for its financial support. The contributions of Mr James Sherwood and Ms Katherine Petros to this research effort are greatly appreciated. The authors would also like to extend their gratitude to Mr Timothy Cline for providing some of the performance data for the Mn/ROAD test sections. Finally, the authors would like to thank Mr Lev Khazanovich for providing the climatic database and information on the traffic data used in this study.

References

- ARA, Inc., 2004. *Guide for mechanistic–empirical design of new and rehabilitated pavement structure*. National Cooperative Highway Research Program, Transportation Research Board, National Research Council, Washington, DC.
- Barenberg, E.J., et al., 2005. *Review comments on the 2002 MEDG for new concrete pavements prepared for NCHRP 1-40A (02)*.
- Beckemeyer, C., Khazanovich, L., and Yu, T., 2002. Determining amount of built-in curling in jointed plain concrete pavement: Case study of Pennsylvania I-80. *Transportation Research Record: Journal of the Transportation Research Board*, 1809, 85–92.
- Burnham, T.R. and Pirkel, W.M., 1997. *Application of empirical and mechanistic empirical pavement design procedures to Mn/ROAD concrete pavement test sections*. Technical Report for Minnesota Department of Transportation, Report No. MN/RC-97/14.
- Byrum, C., 2000. Analysis by high-speed profile of jointed concrete pavement slab curvatures. *Transportation Research Record: Journal of the Transportation Research Board*, 1730, 1–9.
- Coree, B., 2005. *Implementing the mechanistic–empirical pavement design guide: Technical Report*. Iowa State University. Report prepared for the Iowa Highway Research Board (IHRB) Project TR-509.
- Gotlif, A., Mallela, J., and Khazanovich, L., 2006. Finite element study of partial-depth cracks in restrained PCC slabs. *International Journal for Pavement Engineering*, 7 (4), 323–329.
- Gutierrez, J.J., 2008. *Evaluating the JPCP cracking model of the mechanistic–empirical pavement design guide*, Thesis for the Degree Master of Science in Civil Engineering. University of Pittsburgh.
- Hall, K.D. and Beam, S., 2004. Estimating the sensitivity of design input variables for rigid pavement analysis with a mechanistic–empirical design guide. *Transportation Research Record: Journal of the Transportation Research Board*, 1919, 65–73.
- Janssen, D.J. and Snyder, M.B., 2000. Temperature-moment concept for evaluating pavement temperature data. *Journal of Infrastructure Systems. American Society of Civil Engineers*, 6 (2), Technical Note No. 19948.
- Kannekanti, V. and Harvey, J., 2005. *Sensitivity analysis of 2002 design guide rigid pavement distress prediction models*. Davis, CA: University of California. Report prepared for the California Department of Transportation.
- Khazanovich, L. and Yu, T., 2005. Accounting for concrete shrinkage in the mechanistic–empirical pavement design procedure. In: Gilles Pijaudier-Cabot, Bruno Gerard, and Paul Acker, eds. *Creep, shrinkage and durability of concrete structures*. Ecole Centrale de Nantes, France: Hermes Science Publishing, Ltd, 287–292.
- Khazanovich, L., et al., 2001. Development of rapid solutions for prediction of critical CRCP stresses. *Transportation Research Record: Journal of the Transportation Research Board*, 1778, 64–72.
- Khazanovich, L., et al., 2008. Adaption of MEPDG for design of Minnesota low-volume Portland cement concrete pavements. *Transportation Research Record: Journal of the Transportation Research Board*, 2087, 57–67.
- Mu, F., et al., 2010. Prepare and execute a sensitivity analysis to evaluate the MEDPG rigid pavement performance prediction models – task 4 & 5 draft report, FHWA-Project Number DTFH61-05-P-00094.
- Packard, R.G. and Tayabji, S.D., 1985. New PCA thickness design procedure for concrete highway and street pavements. *Proceedings of 3rd International Conference on Concrete Pavement Design and Rehabilitation*, Purdue University.
- Rao, S. and Roesler, J.R., 2005. Characterizing effective built in curling from concrete pavement field measurements. *Journal of Transportation Engineering*, 131 (4), 320–327, American Society of Civil Engineering.
- Vandenbossche, J.M., 2003. *Interpreting falling weight deflectometer results for curled and warped Portland cement concrete pavements*. Thesis for the Degree Doctor of Philosophy in Civil Engineering. University of Minnesota.
- Vandenbossche, J. and Mu, F., 2009. Evaluating the built-in temperature difference in the JPCP cracking model of the MEPDG. *International Journal of Pavement Engineering* (under review).
- Vandenbossche, J.M., et al., 2008. *Sensitivity analysis of various design parameters for JPCPs and CRCPs*. Technical Report for Federal Highway Administration.
- Well, S.A., Phillips, B.M., and Vandenbossche, J.M., 2006. Quantifying built-in construction gradients and early-age slab shape to environmental loads for jointed plain concrete pavements. *International Journal for Pavement Engineers*, 7 (4), 275–289.
- Yu, T., et al., 1998. Analysis of concrete pavement responses to temperature and wheel loads measured from instrumented slabs. *Transportation Research Record: Journal of the Transportation Research Board*, 1639, 94–101.